Method for the hyperspectral inversion of the phosphorus content of rice leaves in cold northern China

Fenghua Yu[1,2], Honggang Zhang[1], Juchi Bai[1], Shuang Xiang[1], Tongyu Xu[1,2*]

(1. *School of Information and Electrical Engineering, Shenyang Agricultural University, Shenyang 110866, China*;
2. *Liaoning Agricultural Information Engineering Technology Research Center, Shenyang 110866, China*)

Abstract: Phosphorus plays a vital role in the growth and development of rice in the cold northern regions, affecting the yield and quality of rice. The phosphorus content of leaves can indicate the nutritional status of rice. Rapid and accurate acquisition of the phosphorus content in leaves is the basis for ensuring healthy rice growth and maintaining stable and high rice yield. Hyperspectral technology can reflect the shape of rice leaves and then evaluate the phosphorus content in the leaves, so hyperspectral technology has the potential to estimate the phosphorus content in plant leaves quickly and accurately. The hyperspectral data of the rice leaves were pretreated using the SG smoothing method. The spectral characteristics of pretreated spectral data were extracted using principal component analysis (PCA) and linear discriminant analysis (LDA). Extreme learning machine (ELM) and Bat algorithm optimized extreme learning machine (BA-ELM) were constructed to retrieve the phosphorus content in rice leaves. The results show that there are seven feature vectors produced by the two methods, and the feature vectors selected by the two methods are used as inputs, respectively. The verification sets R^2 and RMSE of the two models constructed using the feature reflectivity chosen by the LDA algorithm as input were between 0.603 and 0.604, and 0.025 and 0.032, respectively. Under the condition of the same inversion model, the model constructed by using the reflectivity of the features selected by the PCA algorithm as input has a better prediction effect, and the verification set R^2 of the two models was between 0.685-0.765, and RMSE was between 0.022-0.038. In addition, when using the features selected by these two algorithms to model, comparing the prediction results of the two models, it was found that the accuracy of the BA-ELM was higher than that of ELM. Its determination coefficient R^2 and RMSE of the verification set were 0.765 and 0.022, respectively. Because of this, the ELM optimized by principal component analysis and BA has certain advantages in the hyperspectral inversion of phosphorus content in rice leaves in cold regions, and can provide some reference for rapid and accurate detection of phosphorus content in rice leaves.

Keywords: rice, hyperspectral data, phosphorus content, bat algorithm, inversion model
DOI: 10.25165/j.ijabe.20241706.8464

Citation: Yu F H, Zhang H G, Bai J C, Xiang S, Xu T Y. Method for the hyperspectral inversion of the phosphorus content of rice leaves in cold northern China. Int J Agric & Biol Eng, 2024; 17(6): 256–263.

1 Introduction

Phosphorus is an essential element in the morphological composition of various compounds in crops, which participates in many metabolic processes in life and is very important for the growth and development of crops[1]. Adequate phosphorus content will increase the tiller number of rice and improve metabolic function and stress resistance, thus accelerating rice maturation and increasing rice yield. On the contrary, when rice is deficient in phosphorus, the color of the plant becomes dark, the leaves become narrow and even die, and the number of tillers decreases, which affects the development of rice[2]. Research results have shown that a reasonable application rate, application mode, and fertilizer type of phosphate fertilizer could improve the accumulation and transport of dry matter after anthesis, and improve the phosphorus absorption and utilization efficiency of plants[3-5]. However, in actual fertilization, people often choose to apply excessive phosphate fertilizer in pursuit of a high rice yield, leading to the low utilization rate of phosphate fertilizer in the current season. Excess phosphate fertilizer is deposited in the soil. With the increase in the accumulation of phosphate fertilizer, the soil appears to become eutrophic, which will not only lead to a reduction in rice yield but also cause pollution of the non-point source[6]. Therefore, a rapid and accurate diagnosis of the distribution of the phosphorus content in rice leaves is essential to achieve efficient green agriculture[7].

The traditional method for detecting the phosphorus content in rice leaves is chemical analysis. The time and labor cost of chemical analysis is high. Hyperspectral diagnosis of phosphorus content in rice leaves not only can broaden the scope of research on plant phosphorus nutrition diagnosis but also compensate for the disadvantages of traditional phosphorus nutrition diagnosis, which has the advantages of rapidity and non-destructiveness[8,9].

The development of hyperspectral remote sensing technology provides a new means of rapid and non-destructive monitoring of crop components[10]. UAV hyperspectral images were used to estimate different nitrogen traits of leaf nitrogen content (LNC), plant nitrogen content (PNC), leaf nitrogen accumulation (LNA), and plant nitrogen accumulation (PNA). Additionally, the influence of the growth stage was evaluated. The results showed that the

Received date: 2023-08-01 **Accepted date:** 2024-10-13
Biographies: **Fenghua Yu**, PhD, Professor, research interest: precision agricultural aviation and radiative transfer modeling research, Email: adan@syau.edu.cn; **Honggang Zhang**, Master dissertation, research interest: UAV remote sensing research, Email: a961972679@163.com; **Juchi Bai**, PhD candidate, research interest: 3D radiative transfer modeling research. Email: 773858526@qq.com; **Shuang Xiang**, PhD candidate, rearch interest: leaf radiative transfer mechanisms research, Email: 3405514229@qq.com.
***Corresponding author: Tongyu Xu**, PhD, Professor, research interest: precision agricultural aviation research. School of Information and Electrical Engineering, Shenyang Agricultural University, Shenyang 110866, China. Tel: +86-13940021960, Email: xutongyu@syau.edu.cn.

correlation between four nitrogen traits and three biochemical traits - leaf chlorophyll content, canopy chlorophyll content, and aboveground biomass - was affected by the growth stage. Tian et al.[11,12] estimated LNC in rice under variable vegetation cover by constructing a spectral index. The results showed that this was the best index for estimating LNC in rice under various cultivation conditions. The canopy nitrogen status of rice was estimated by binary Particle Swarm Optimization-support vector regression (BPSO-SVR) using hyperspectral reflectance in the cold regions. The results showed that the BPSO-SVR method had an excellent RMSE (0.913-0.949) and a small RMSE (0.055-0.127) in fitting the canopy nitrogen concentration of rice in three stages of growth. Liu et al.[13] analyzed hyperspectral reflectance data based on wavelet analysis to monitor the stress level of rice polluted with heavy metals. The results showed that the red edge position (REP) was the most sensitive index to monitor the level of rich metal pollution in rice crops.

It can be seen that a great deal of research has been carried out on the detection of nitrogen content in wheat[14], rice, corn[15], and other crops by hyperspectral technology. However, there are relatively few studies on the detection of phosphorus content. Mahajan et al.[16] and others used hyperspectral remote sensing technology to monitor the contents of nitrogen, phosphorus, sulfur, and potassium in wheat and evaluated the predictability of plant N-P-S-K for eight traditional vegetation indices (VIs) and three proposed vegetation indices (1 P and 2 S). The results showed that the P content predicted by VI ($P_{1080\text{-}1460}$) had high precision (correlation coefficient R^2=0.42). Mutanga et al.[17] used hyperspectral image data to estimate and map the distribution of phosphorus concentration in African prairie grass. The results showed that the best-trained neural network predicted the phosphorus distribution with a determination coefficient of 0.63 and a root mean square error (RMSE) of 0.07, and the absorption characteristics located in the short-wave infrared ($R_{2015\text{-}2199}$) contained more information about the phosphorus distribution.

In summary, hyperspectral technology can perform rapid and accurate detection of phosphorus content in rice leaves. It is of great significance to quickly ascertain the growth status of rice, but scholars at home and abroad have relatively little research on the inversion of the phosphorus content in rice by hyperspectral technology, and the basis for reference is still minimal. Therefore, to further solve the problem of excessive application of phosphorus fertilizer, and to improve the precision and applicability of the inversion of the phosphorus content in rice leaves, this study took rice as the research object, analyzed the hyperspectral changes in rice leaves under phosphorus stress, and established a hyperspectral inversion model of the phosphorus content in rice leaves in cold northern China, and could be used as a reference for precise fertilization and field management of rice.

2 Experimental part

2.1 Experimental design

The experiment was conducted from June to September 2021 in the experimental rice base of Shenyang Agricultural University (122°43′33″E and 40°58′44″N), Haicheng City, Anshan City, Liaoning Province. The rice variety was Beijing 1705. The experimental rice field was divided into 11 plots as shown in Figure 1, with five nitrogen fertilizer gradients. The nitrogen fertilizer application rates were as follows: N_0=0, N_1=50 kg/hm^2, N_2=100 kg/hm^2, N_3=150 kg/hm^2, N_4=200 kg/hm^2. Due to the effect of the interaction between nitrogen and phosphorus absorption in rice leaves[18], the phosphorus content (LPC) of rice varied with the amount of nitrogen fertilizer applied, so there was no phosphorus fertilizer gradient in the experiment. The amount of phosphorus fertilizer involved in each plot was 1080 kg/hm^2, and the other management measures were the same.

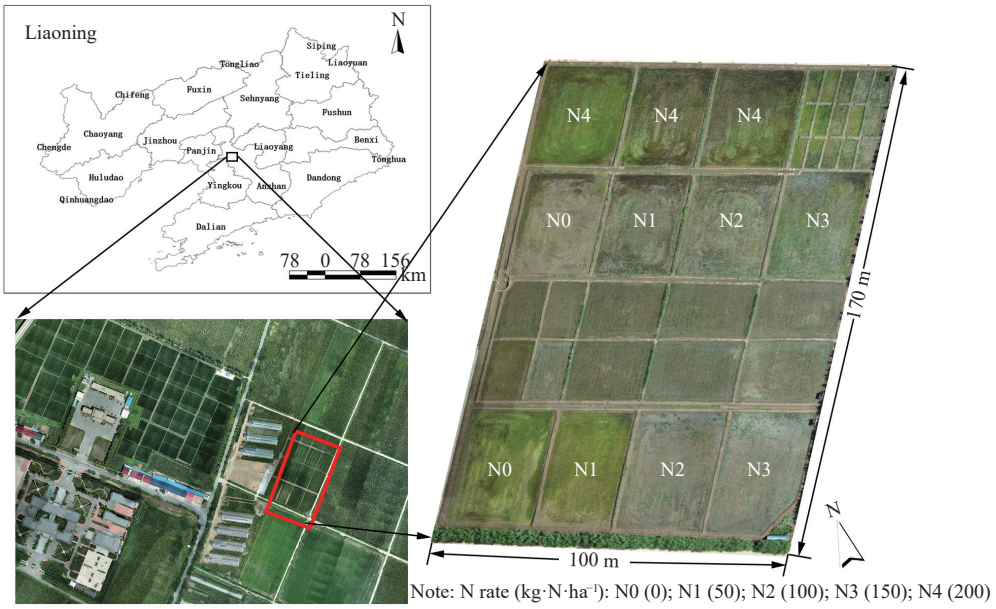

Note: N rate (kg·N·ha^{-1}): N0 (0); N1 (50); N2 (100); N3 (150); N4 (200)

Note: Figure created in SuperMap 11i (supermap.com), made with RiverMap (www.rivermap.cn).

Figure 1 Plot distribution of the experimental field

The entire rice growth period was sampled since June 2021. The sampling interval was seven days, and the sampling process was as follows: Prepare self-sealing bags before sampling and mark them according to plots. Randomly select three rice holes as sample points in each property of the experimental field for destructive sampling. Put the selected samples in self-sealing bags and bring them back to the laboratory, remove the roots, keep the leaves, deactivate the enzymes at 105°C for 2 h, dry them at 90°C at low

temperature, and weigh and crush them after drying. Put the crushed samples in labeled envelopes and store them in a drying vessel.

2.2 Extraction of spectral information from rice leaves

The spectral data of the rice leaves in this study were obtained using an HR2000+ spectrometer, and the spectral reflectance was collected using Ocean View software. The spectrometer was manufactured by Ocean Optics Company of America. The spectral range of HR2000+ is 400-1000 nm, and its resolution is 0.4610 nm. Before the spectrum of the sample was collected, the instrument was corrected using its whiteboard. To reduce the error, whiteboard correction was carried out strictly every 10 min. When collecting leaf spectral data, the probe must be tightly attached to the blade to avoid interference caused by sunlight and other factors[19].

2.2.1 Determination of phosphorus concentration in rice leaves

The method for detecting phosphorus concentration in rice leaves is vanadium molybdenum yellow colorimetry. Before determination, impurities were removed from the ground sample, the 0.3-0.4 g sample was weighed, and then placed in a conical flask. The mixture of water, sulfuric acid, and perchloric acid-nitric acid was added for digestion and then placed in a volumetric flask as the solution to be calculated. Part of the solution to be measured was put in a 50 mL volumetric flask, dinitrophenol indicator and sodium hydroxide solution were added, and the solution was mixed until its color turned yellow. After modulation, ammonium vanadium molybdate chromogenic agent and water were added for a constant volume. After some time, the spectrophotometry of the solution was measured with a cuvette, and the phosphorus content was calculated according to the absorbance value[20].

2.2.2 Spectral data preprocessing

Because of baseline drift, sample inhomogeneity, scattering, and artificial operation, the spectral signal contains a small amount of noise in the process of hyperspectral data acquisition. To obtain more accurate and effective spectral information, the advantages and disadvantages of various spectral pretreatment methods were compared. In this study, an outlier removal method based on linear interpolation and SG smoothing was proposed. Because SG smoothing does not change the shape or width of the signal when filtering noise, the correlation between spectral reflectivity and phosphorus content was enhanced. Therefore, the two methods were combined to reduce the noise from spectral data.

2.2.3 Extraction of spectral characteristics of rice leaves

After preprocessing, the spectral data are still a high-dimensional dataset. There is a lot of redundancy and a strong correlation between the spectral bands, so the subsequent processing is complex. Therefore, the selection of features from the rice leaf spectral data is the key to improving the accuracy of the model. Principal component analysis (PCA) and linear discriminant analysis (LDA) were used in this study.

2.2.4 Principal component analysis

PCA is to recombine several characteristic indices that can reflect the phosphorus application level of rice. A group of unrelated and non-overlapping comprehensive indices was formed to replace the original influence indices. Some extensive indices which could reflect the original index information were extracted according to the actual demand, to accurately predict and classify the rice phosphorus level. The norm value is the length of the vector norm of the index in the multidimensional space composed of principal components. The longer the distance, the greater the total load of the index on all main components, and the stronger its ability to interpret complete information. The norm value is calculated by:

$$N_{ik} = \sqrt{\sum_{i=1}^{k} (U_{ik}^2 \lambda_k)} \quad (1)$$

where, N_{ik} is the comprehensive load of the i^{th} variable in the first k principal components with eigenvalue >1; U_{ik} is the load of the i^{th} variable in the k^{th} principal component; and λ_k is the eigenvalue of the k^{th} principal component[21].

2.2.5 Linear discriminant analysis

LDA is used to maximize the ratio between different classes and conflicts of the same type. To achieve the maximum separation between feature sets in each category, for K-class LDA, the sample space is divided into K classes, each class is composed of a specific number of data samples corresponding to the same phosphorus type, and the K-class linear discriminant function is as in Equation (2):

$$C_j(X_j) = v_j^{\mathrm{T}} X_j + v_{h0} = v_{j1} x_{j1+} v_{j2} x_{j2} + \ldots + v_{jD} x_{jD} + v_D \quad (2)$$

where, j=1, 2, 3, …, k−1; X_j=[x_{j1}, x_{j2}, x_{j3}, …, x_{jD}] is the D-dimensional vector of the jth sample; $v_j^{\mathrm{T}} = [v_{j1}, v_{j1}, \ldots, v_{jD}]$ is the coefficient matrix of class j; v_{j0} is the threshold of class j sample classification.

In the training stage, the weighting coefficient matrix is obtained from the training samples in the iterative process. For each training sample X_i belonging to class i, the coefficient matrix is obtained by training so that $C_i(X_i)$ is larger than all other classes. To classify unknown samples, the weighting coefficients calculated in the training stage will be used to calculate the X_i discriminant function of test samples. A test sample can be divided into a class of linear discriminant functions if the class of linear discriminant functions of the test sample is more significant than any other class of linear discriminant functions. If Equation (3) is satisfied, the test sample belongs to class O[22].

$$C_O(X_i) \geq C_q(X_i), \ \forall o \neq q \quad (3)$$

2.3 Modeling method

2.3.1 Extreme learning machine

ELM is a kind of model proposed by Huang et al.[23], with the advantages of simple operation, fast training speed, and less human intervention. The model randomly selected the weight of the input layer and the offset of the hidden layer during initialization. The importance of the output layer was calculated analytically by minimizing the loss function composed of the training error term and the regular time of the weight norm of the output layer according to the Moore-Penrose (MP) generalized inverse matrix theory. It does not need to be adjusted in the training modeling process, so it is not necessary to manually change the number of neurons in the hidden layer to find the optimal prediction value. From the aspect of learning efficiency, the ELM learning process is not only simple but also efficient, but the process of randomly generating initial values quickly leads to a decrease in stability and generalization of the created model[24,25].

2.3.2 Extreme learning machine optimized by bat algorithm

The Bat algorithm (BA) is a heuristic search algorithm based on swarm intelligence proposed by Yang[26] in 2010. It is an effective method to search for the optimal global solution. The algorithm is an optimization technique based on iteration, which initializes a set of random keys, then searches for the optimal solution through iteration, and generates a new local solution by random flight around the optimal solution, thus strengthening the local search. To improve the inversion accuracy of the ELM method, the bat algorithm is used to optimize the input layer

parameters and the hidden layer of the ELM network. Using the global optimization ability of the bat algorithm, the optimal input layer weight and invisible layer threshold of ELM were obtained, thus avoiding the defect of the diagnostic190 accuracy of ELM not being high enough due to poor parameter selection. The flow chart of the BA algorithm optimizing the parameters of the ELM model is shown in Figure 2.

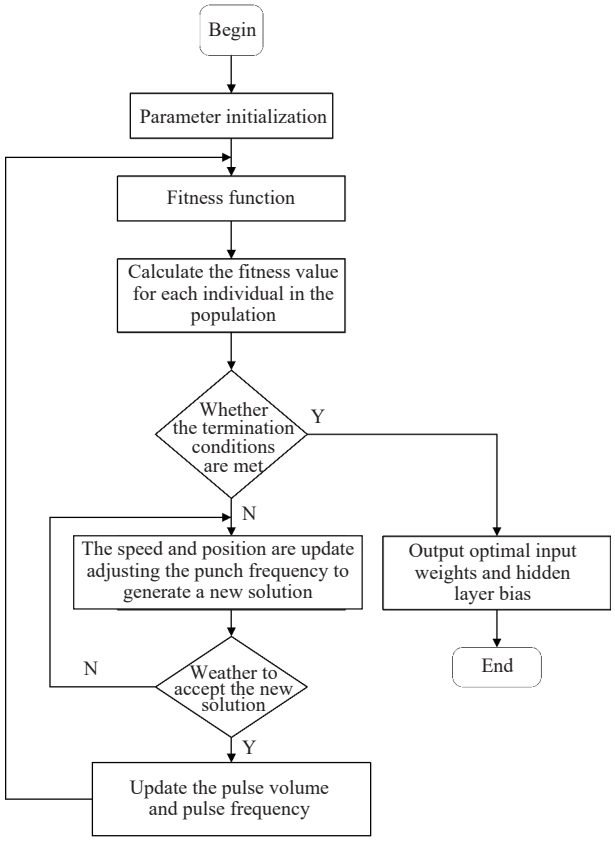

Figure 2 Chart of ELM optimization based on BA

Suppose that there are N arbitrary samples (X_i, t_i), where, $X_i=(x_{i1}, x_{i2}, x_{i3}, \ldots, x_{in})^T \in R^n$, $t_i=(t_{i1}, t_{i2}, \ldots, t_{in})^T \in R^m$, n is the dimension of the input layer, m is the dimension of the output layer, $g(x)$ is the activation function, and the number of nodes in the hidden layer is L. The main process of optimizing ELM model parameters by the BA algorithm is as follows:

Step 1: Initialization parameters: the maximum number of iterations N_iter=50, the initial population number N_pop=20, the maximum pulse volume A_0=1.6 and the maximum pulse rate r_0=0.0001, the search pulse frequency range $[f_{min}, f_{max}]$=[0, 2], the attenuation coefficient α=0.9, the enhancement coefficient γ=0.99;

Step 2: Randomly initializing the bat position Y_i, which is composed of the input layer weight Y_i and the hidden layer bias b_i of the ELM network; calculating the node output matrix $\boldsymbol{H}$ of the hidden layer; and determining the corresponding output weight β;

Step 3: The design of the fitness function. The root mean square error of the classification results is used as the fitness function of the BA algorithm, and its expression is Equation (4). In the evolution process, the individual with the smallest fitness is selected as the current optimal solution;

$$fitness = \sqrt{\frac{\sum_{i=1}^{N}\sum_{j=1}^{L}\beta_j g(W_j \cdot X_i + b_j) - t_i^2}{mN}} \quad (4)$$

Step 4: Adjust the search pulse frequency of bats, update the speed and position, and obtain the next generation population;

Step 5: Judge whether the termination condition is satisfied; if so, the output ELM parameters correspond to the optimal global position of the bat (input weight W_i and hidden layer bias b_i, otherwise return to Step 2 and repeat Steps 2-5).

3 Results

3.1 Data preprocessing and phosphorus statistics

The sampling data were pretreated by the SG smoothing spectral processing method. The results are shown in Figure 3. The standard deviation method was adopted three times to eliminate outliers in the samples, 253 valid samples were obtained, the SPXY algorithm was used to divide the training set and the verification set for valid samples, and 184 training sets groups and 69 verification sets groups were obtained. The statistical results of the phosphorus concentration are listed in Table 1. From Figure 4, the average value of the sample data is 0.3305 mg/g, the maximum value is 0.403 mg/g, the minimum value is 0.216 mg/g, and the standard deviation is 0.0371 mg/g. Therefore, it can be seen that of the phosphorus content data of 253 groups of rice leaves in this study, 200 conform to a normal distribution, which can support the following research.

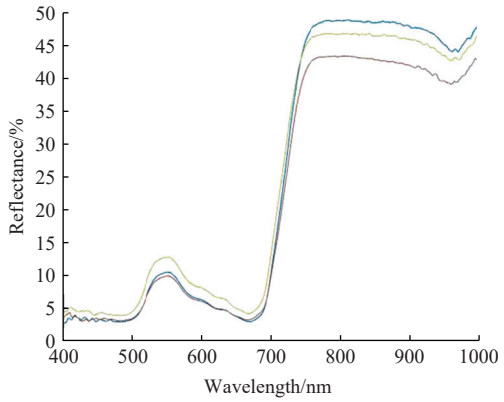

Figure 3 SG smooth spectral curve

Table 1 Dataset statistics of phosphorus content in rice leaves

Dataset	Sample size/piece	Average/ mg·g^{-1}	Maximum value/mg·g^{-1}	Minimum value/mg·g^{-1}	Standard deviation/mg·g^{-1}
Training set	184	0.3318	0.403	0.216	0.0401
Verification set	69	0.3271	0.372	0.249	0.0274

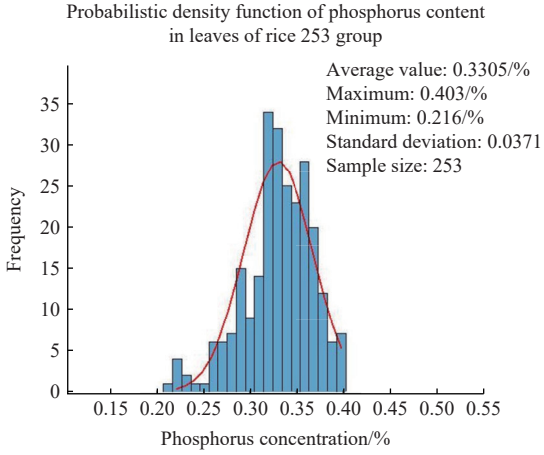

Figure 4 Probability density function of phosphorus content in leaves of rice group 253

3.2 Feature extraction

3.2.1 Correlation analysis of rice leaf spectral reflectance with P

In this study, the correlation between hyperspectral reflectance and P of rice was analyzed, and the results of the analysis are shown in Figure 5. The correlation between hyperspectral reflectance and S was positive at 400-770 nm and negative at 770-1000 nm. It was higher at 530-630 nm and 700-720 nm, with a maximum of 0.1392. The correlation curves were similar to those of nitrogen, which may be due to the similarity of the principles of the effects of N and P on the hyperspectral reflectance of rice leaves. Considering the poor correlation of S to the original hyperspectral bands, in this study, PCA was used to extract features from the hyperspectral data before inverse modeling.

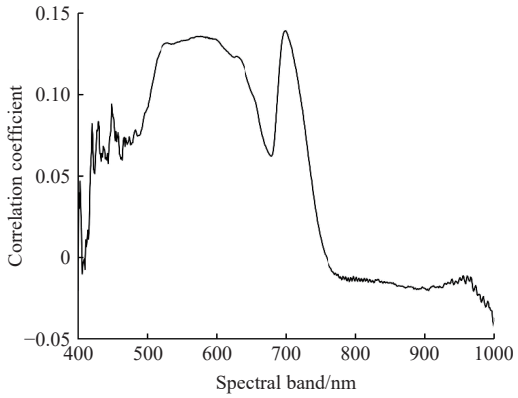

Figure 5 Correlation between P and hyperspectral reflectance in rice

3.2.2 Feature selection by principal component analysis

In this study, PCA dimension reduction was used to transform multiple indicators into a few indicators, eliminating the correlation among many indicators and making them irrelevant. PCA can project data to several orthogonal directions with the most significant variance to retain the most sample information. The greater the conflict of samples, the better the diversity of samples. Figure 6 is the scatter plot of each vector after PCA dimensionality reduction. The circle of each color represents a group of vectors with high similarity. If the points of several samples are gathered together, the similarity between these samples is very high; on the contrary, if several sample points are very scattered, the similarity between these samples is relatively low. In this study, the PCA algorithm was used to project the data into an orthogonal subspace with microscopic dimensions, which eliminates redundant information between adjacent highly correlated frequency bands. Pearson correlation analysis was carried out on the data after PCA dimension reduction, and the analysis results are shown in Figure 7. It can be seen that the correlation coefficient between each principal component is less than 0.1098, which is used as a characteristic of the inversion of the phosphorus content.

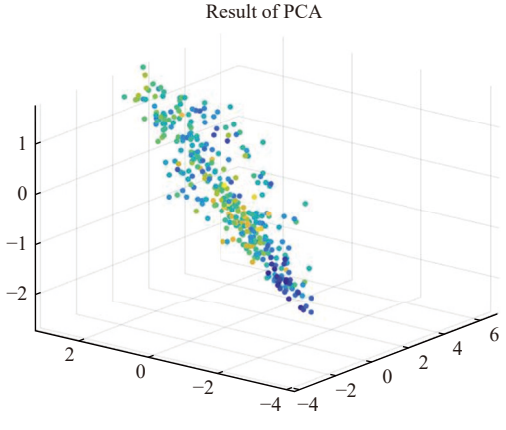

Figure 6 PCA dimensionality reduction result plot

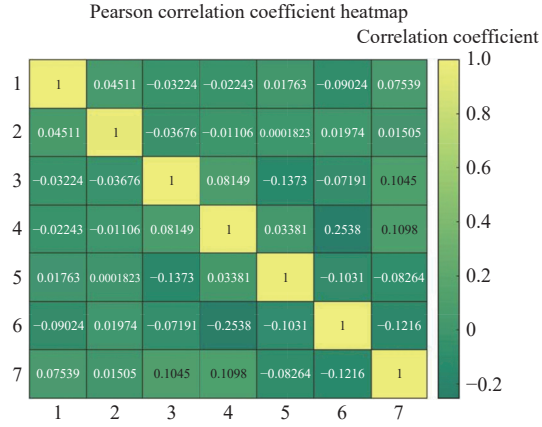

Figure 7 Pearson correlation analysis results plot

3.2.3 Feature selection by linear discriminant analysis

LDA aims to search for multiple discriminant vectors to maximize the ratio of interclass distance to intraclass distance. In this study, the LDA method in the toolbox is used to reduce the dimension of spectral data. Figure 8 shows the resulting diagram after LDA dimension reduction, in which various circles of different colors represent vectors that maximize the distance between classes. Finally, seven sets of feature vectors are selected for phosphorus inversion modeling[27-28].

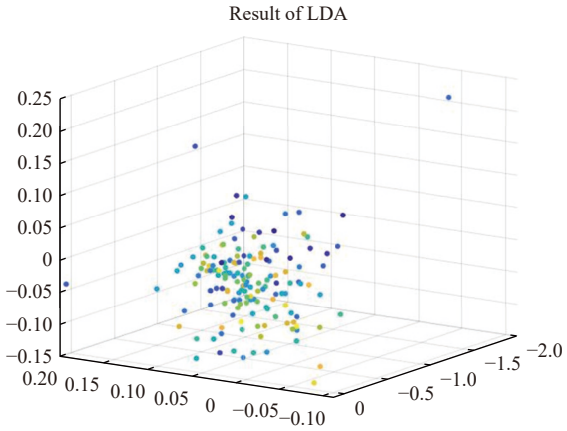

Figure 8 LDA dimensionality reduction scatter plot

3.3 Inversion modeling and analysis of phosphorus content in rice leaves

3.3.1 Inversion modeling of extreme learning machine

In this study, the training samples obtained by PCA and LDA after reducing the data dimension were used as input to the ELM model. Measured values of phosphorus concentration in rice leaves were used as training results, and the ELM network was trained. After continuous attempts, the parameters of ELM were set as follows: the output function was Purelin, the training function was the trail, the activation function was Sigmoid, and the number of hidden layer nodes was 25. The final results of the inversion are shown in Figure 9.

As can be seen from Figure 9, compared with the two-dimensionality reduction methods, the model established by using the feature vector obtained by the PCA algorithm as the input of the ELM model is more effective, with R^2 reaching 0.703 and 0.685 and

RMSE reaching 0.022 and 0.038 mg/g, respectively. However, the ELM model established by linear discriminant analysis is not effective, since the R^2 of the model reaches 0.609 and 0.603, and the RMSE is 0.025 and 0.025 mg/g, respectively.

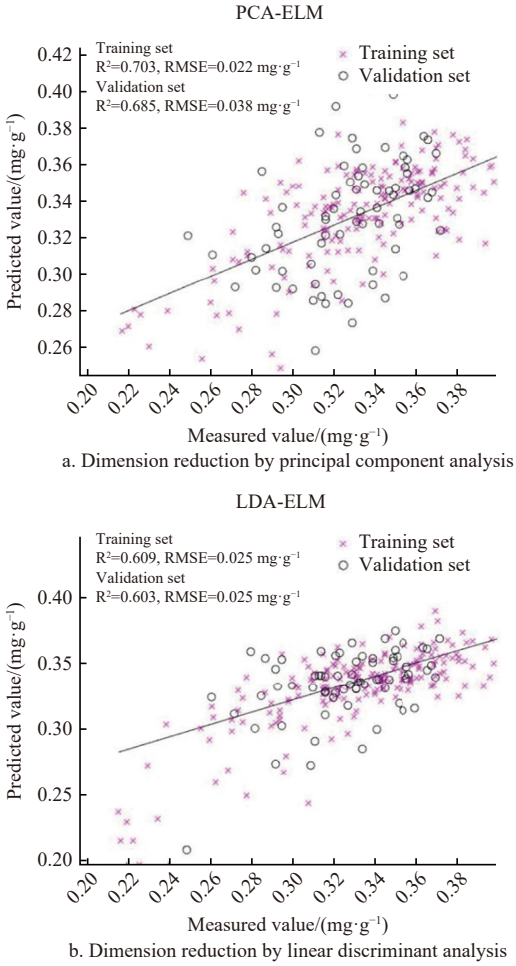

a. Dimension reduction by principal component analysis

b. Dimension reduction by linear discriminant analysis

Figure 9 Inversion results of rice leaf phosphorus concentration estimation model based on ELM

3.3.2 Extreme machine learning inversion modeling for optimizing bat algorithm

The input parameters of the prediction model established by BA-ELM are as follows: the number of nodes in the input layer is set to 5, the number of nodes in the hidden layer is set to 80, the activation function is sigmoidal, and the bias between the input layer and the hidden layer is optimized by the BA algorithm, to optimize the BA-ELM network. Inversion results are shown in Figure 10.

It can be seen from Figure 10 that the inversion effect of the ELM model optimized by the bat algorithm on rice phosphorus concentration is significantly better than that of the traditional ELM algorithm. The BA-ELM model established by using feature vectors obtained by principal component analysis has the highest accuracy, and the training set and verification set R^2 of the model reach 0.805 and 765, respectively, and RMSE are 0.019 and 0.022 mg/g, respectively. The inversion accuracy of the BA-ELM model established by linear discriminant analysis is low. The training set and the verification set of the model reach 0.729 and 0.604, respectively, and the RMSE is 0.022 and 0.032 mg/g, respectively.

3.4 Thematic maps of rice P content based on inversion results of different algorithms

The measured hyperspectral data of 7.30 after PCA feature

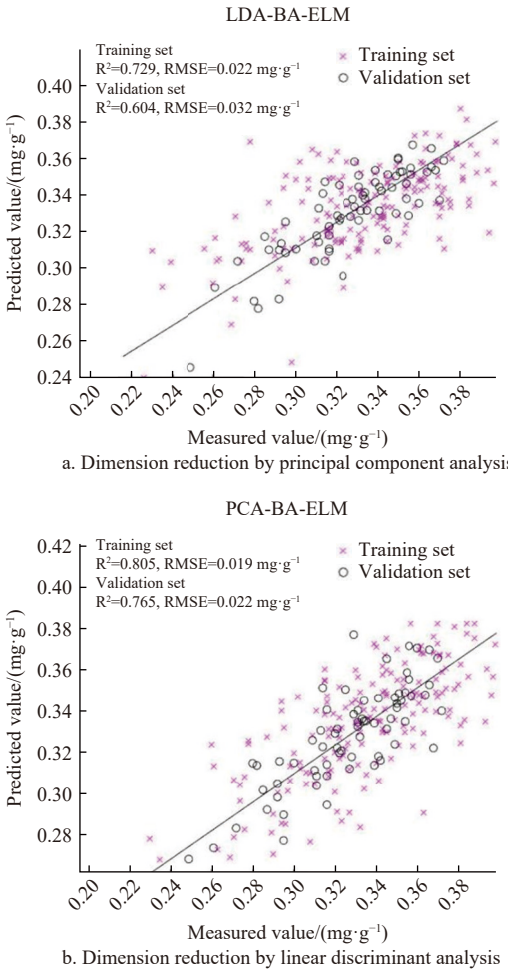

a. Dimension reduction by principal component analysis

b. Dimension reduction by linear discriminant analysis

Figure 10 Inversion results of rice leaf phosphorus concentration estimation model based on BA-ELM

extraction were selected, in the inversion results of different algorithms, and the thematic maps of the inversion results of rice P content were plotted. As shown in Figure 11, overall, the inversion results of the two algorithms were closer to the actual fertilizer application, and the accuracy of the BA-ELM model was due to the ELM model. However, there was an overestimation of S content in some plots, which might be due to the fact that there were more data in the high N fertilizer plots, and under the influence of N and P synergism, there were more data with high S content, which led to high model fitting results.

4 Discussion

The results of the rice phosphorus inversion models established by ELM and BA-ELM were compared and analyzed, and the evaluation indices of the two models are listed in Table 2.

It can be seen in Table 2 that, in this study, compared to the LDA algorithm, the PCA algorithm is more advantageous in constructing the inversion model of the phosphorus content in rice leaves. By comparing the results of the ELM model and the BA-ELM model, it is found that the prediction effect of BA-ELM is higher, regardless of whether the reflectivity of features used as the input is selected by the PCA algorithm or the LDA algorithm, and the training set R^2 of the model is improved by 0.102. The verification set R^2 is improved by 0.08. The reason may be that ELM is a generalized machine learning method of a single hidden layer feedforward neural network, in which the connection weights between the input layer and the hidden layer and the threshold of

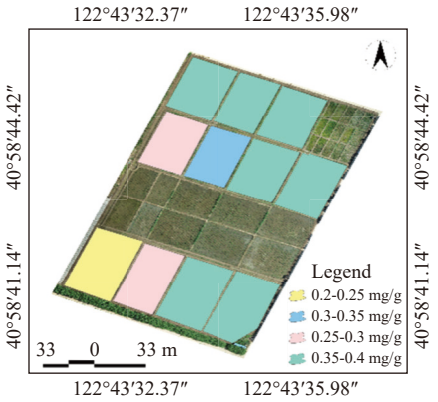

a. Pcontent thematic maps based on ELM

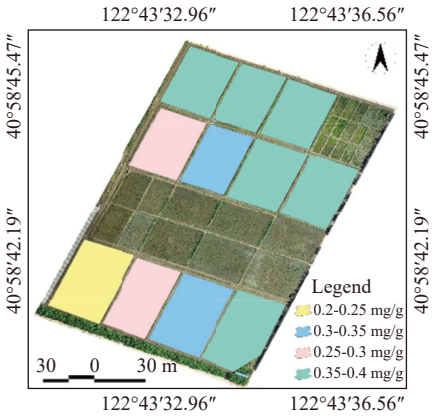

b. Thematic maps of P content based on BA-ELM

Figure 11 Thematic maps of rice P content based on the inversion results of different algorithms

Table 2 Evaluation indices of ELM and BA-ELM inversion models

Feature extraction method	Inversion model	R^2		RMSE	
		Training set	Verification set	Training set	Verification set
PCA	ELM	0.703	0.685	0.022	0.038
LDA	ELM	0.609	0.603	0.025	0.025
PCA	BA-ELM	0.805	0.765	0.019	0.022
LDA	BA-ELM	0.729	0.604	0.022	0.032

the hidden layer are randomly generated, and there is no need to adjust in the training process. Although it can avoid the tedious iterative adjustment of neural network parameters, it easily falls into optimal local solutions[29,30]. Bat algorithm can not only maximize the global and regional search ability of BA and the advantages of fast learning of ELM but also overcome the inherent instability of ELM, which makes the algorithm converge faster and diagnose more accurately.

It is undeniable that this study still has deficiencies in experimental design and data collection. Due to the limitation of the experimental equipment, the collected hyperspectral data and P data were both leaf-scale rather than canopy-scale data, which caused some obstacles to the application of the model in real production environments. At the same time, due to the lack of a radiative transfer model that includes P, the study adopted a data-driven approach for modeling, and although the model achieved high inversion accuracy, the model's ability to generalize still needs to be validated in further studies. Future research is planned to conduct a study on rice P inversion based on UAV hyperspectral data at the canopy scale so that the model can be more widely used in agricultural production.

5 Conclusions

In this study, the spectral data of the rice leaves were measured by marine optical HR2000+, and the phosphorus concentration of the rice leaves was measured by vanadium molybdenum yellow colorimetry. The inverse results of the PCA and LDA, ELM, and BA-ELM models were compared and analyzed, and the following conclusions were obtained:

1) Two methods, PCA and LDA, were used to extract hyperspectral features from rice leaves, and seven vectors of characteristics were extracted.

2) Under the same model prediction condition, when the features selected by the PCA algorithm were used as input, the training set R^2 of the model was 0.076 higher than that of the LDA algorithm. The verification set R^2 was 0.160 higher than that of the LDA algorithm, which proves the superiority of the PCA algorithm in extracting spectral features of rice leaves and establishing an inversion model.

3) Compared to ELM, the BA-ELM model has a better inversion effect; R^2 of the training set was 0.8053, which is improved by 0.102, and R^2 of the verification set was 0.7647, which is improved by 0.0802. Therefore, the optimization of the ELM network by the bat algorithm can improve the inversion effect to a certain extent.

Acknowledgements

This work was financially supported by the General Program of Natural Science Foundation of Liaoning Province of China (Grant No. 2023-MSLH-283), the Platform Program of Education Department of Liaoning Province (Grant No. JYTPT2024002), and the Liaoning Province "Xingliao Talent Program" Project (Grant No. XLYC2203005). The authors acknowledge the Liaoning Provincial Department of Education and the School of Information and Electrical Engineering of Shenyang Agricultural University for their support.

[References]

[1] Ramoelo A, Skidmore A K, Cho M A, Mathieu R, Heitkonig I M A, Dudeni-Tlhone N, et al. Non-linear partial least square regression increases the estimation accuracy of grass nitrogen and phosphorus using *in situ* hyperspectral and environmental data. ISPRS Journal of Photogrammetry and Remote Sensing, 2013; 82: 27–40.

[2] Siedliska A, Baranowski P, Pastuszka-Woźniak J, Zubik M, Krzyszczak J. Identification of plant leaf phosphorus content at different growth stages based on hyperspectral reflectance. BMC Plant Biology, 2021; 21: 28.

[3] de Oliveira K M, Furlanetto R H, Rodrigues M, dos Santos G L A A, Reis A S, Crusiol L G T, et al. Assessing phosphorus nutritional status in maize plants using leaf-based hyperspectral measurements and multivariate analysis. International Journal of Remote Sensing, 2022; 43(7): 2560–2580.

[4] Song X, Xu D Y, Huang C C, Zhang K K, Huang S M, Guo D D, et al. Monitoring of nitrogen accumulation in wheat plants based on hyperspectral data. Remote Sensing Applications: Society and Environment, 2021; 23: 100598.

[5] Lu J S, Li W Y, Yu M L, Zhang X B, Ma Y, Su X, et al. Estimation of rice plant potassium accumulation based on non-negative matrix factorization using hyperspectral reflectance. Precision Agriculture, 2021; 22(1): 51–74.

[6] Cao Y L, Jiang K L, Wu J X, Yu F H, Du W, Xu T Y. Inversion modeling of japonica rice canopy chlorophyll content with UAV hyperspectral remote sensing. PloS One, 2020; 15(9): e0238530.

[7] Liu W, Sun C F, Zhao Y N, Xu F, Song Y L, Fan J R, et al. Monitoring of wheat powdery mildew under different nitrogen input levels using hyperspectral remote sensing. Remote Sensing, 2021; 13(18): 3753.

[8] Li T S, Zhu Z, Cui J, Chen J H, Shi X Y, Zhao X, et al. Monitoring of leaf nitrogen content of winter wheat using multi-angle hyperspectral data.

International Journal of Remote Sensing, 2021; 42(12): 4672–4692.

[9] Tian Y C, Yao X, Yang J, Cao W X, Zhu Y. Extracting red edge position parameters from ground-and space-based hyperspectral data for estimation of canopy leaf nitrogen concentration in rice. Plant Production Science, 2011; 14(3): 270–281.

[10] Wang L, Chen S S, Li D, Wang C Y, Jiang H, Zhang Q, et al. Estimation of paddy rice nitrogen content and accumulation both at leaf and plant levels from UAV hyperspectral Imagery. Remote Sensing, 2021; 13(15): 2956.

[11] Tian Y C, Gu K J, Chu X, Yao X, Cao W X, Zhu Y. Comparison of different hyperspectral vegetation indices for canopy leaf nitrogen concentration estimation in rice. Plant and Soil, 2014; 376(1): 193–209.

[12] Tan K Z, Wang S W, Song Y Z, Liu Y, Gong Z P. Estimating nitrogen status of rice canopy using hyperspectral reflectance combined with BPSO-SVR in cold region. Chemometrics and Intelligent Laboratory Systems, 2018; 172: 68–79.

[13] Liu M L, Liu X N, Ding W C, Wu L. Monitoring stress levels on rice with heavy metal pollution from hyperspectral reflectance data using wavelet-fractal analysis. International Journal of Applied Earth Observation and Geoinformation, 2011; 13(2): 246–255.

[14] Guo B B, Qi S L, Heng Y R, Duan J Z, Zhang H Y, Wu Y P, et al. Remotely assessing leaf N uptake in winter wheat based on canopy hyperspectral red-edge absorption. European Journal of Agronomy, 2017; 82 (Part A): 113–124.

[15] Strachan I B, Pattey E, Boisvert J B. Impact of nitrogen and environmental conditions on corn as detected by hyperspectral reflectance. Remote Sensing of Environment, 2002; 80(2): 213–224.

[16] Mahajan G R, Sahoo R N, Pandey R N, Gupta V K, Kumar D. Using hyperspectral remote sensing techniques to monitor nitrogen, phosphorus, sulphur and potassium in wheat (*Triticum aestivum* L.). Precision Agriculture, 2014; 15(5): 499–522.

[17] Mutanga O, Kumar L. Estimating and mapping grass phosphorus concentration in an African savanna using hyperspectral image data. International Journal of Remote Sensing, 2007; 28(21): 4897–4911.

[18] Ball K R, Liu H, Brien C, Berger B, Power S A, Pendall E. Hyperspectral imaging predicts yield and nitrogen content in grass-legume polycultures. Precision Agriculture, 2022; 23: 2270–2288.

[19] Chen S M, Hu T T, Luo L H, He Q, Zhang S W, Lu J S. Prediction of nitrogen, phosphorus, and potassium contents in apple tree leaves based on in-situ canopy hyperspectral reflectance using stacked ensemble extreme learning machine model. Journal of Soil Science and Plant Nutrition, 2022; 22: 10–24.

[20] Guo P T, Shi Z, Li M F, Luo W, Cha Z Z. A robust method to estimate foliar phosphorus of rubber trees with hyperspectral reflectance. Industrial Crops and Products, 2018; 126: 1–12.

[21] Farrell M D, Mersereau R M. On the impact of PCA dimension reduction for hyperspectral detection of difficult targets. IEEE Geoscience and Remote Sensing Letters, 2005; 2(2): 192–195.

[22] Bandos T V, Bruzzone L, Camps-Valls G. Classification of hyperspectral images with regularized linear discriminant analysis. IEEE Transactions on Geoscience and Remote Sensing, 2009; 47(3): 862–873.

[23] Yi Q X, Huang J F, Wang F M, Wang X Z, Liu Z Y. Monitoring rice nitrogen status using hyperspectral reflectance and artificial neural network. Environmental Science & Technology, 2007; 41(19): 6770–6775.

[24] Ye A S, Zhou X B, Miao F. Innovative hyperspectral image classification approach using optimized CNN and ELM. Electronics, 2022; 11(5): 775.

[25] Singh M, Chauhan S. A hybrid-extreme learning machine based ensemble method for online dynamic security assessment of power systems. Electric Power Systems Research, 2023; 214: 108923.

[26] Yang X. A new metaheuristic bat-inspired algorithm. In: Nature Inspired Cooperative Strategies for Optimization (NICSO). 2010; pp.65–74. doi: 10.1007/978-3-642-12538-6_6.

[27] Xia C, Yang S, Huang M, Zhu Q B, Guo Y, Qin J W. Maize seed classification using hyperspectral image coupled with multi-linear discriminant analysis. Infrared Physics & Technology, 2019; 103: 103077.

[28] Prendergast L A, Smith J A. Influence functions for linear discriminant analysis: Sensitivity analysis and efficient influence diagnostics. Journal of Multivariate Analysis, 2022; 190: 104993.

[29] Huang G B, Zhu Q Y, Siew C-K. Extreme learning machine: A new learning scheme of feedforward neural networks. IEEE International Joint Conference on Neural Networks, Budapest, 2004; pp.985–990. doi: 10.1109/ijcnn.2004.1380068.

[30] Singh M, Chauhan S. A hybrid-extreme learning machine based ensemble method for online dynamic security assessment of power systems. Electric Power Systems Research, 2023; 214(Part B): 108923.